Leopold-Franzens-Universität Innsbruck

Fortgeschrittenen Praktikum III, Instruction: Noise measurements

Gerhard Kirchmair *
Michael Schmid †

Innsbruck, April 5, 2016
Version 3.0

*Gerhard.Kirchmair@uibk.ac.at
†m.schmid@student.uibk.ac.at

Contents

1. Abstract

In this experiment, the behaviour of fundamental electronic noise sources in the form of thermal Johnson noise and shot noise is examined. The measurements are performed in a setup that provides the control of bandwidth and large enough amplification to measure the small noise signals and at the same time maintain a sufficient signal to noise ratio. The two types of noise are characterised by their dependence on the measurement bandwidth and the magnitude of the quantity that acts as the noise source. In case of Johnson noise this is the resistance of a probe, whereas for shot noise this quantity is represented by the photocurrent created by a illuminated photodiode. In a final experiment, the two noise sources are combined to implement a simple noise thermometry measurement with the aim of determining the temperature of liquid nitrogen.

2. Introduction

In most measurement setups, noise represents a detrimental and unwanted disturbance of an underlying process that is analysed. In a best-case scenario, this influence is simply averaged out if the integration time or number of measurements is increased to a certain level. However, if the signal-to-noise ratio is too low, the time scales needed to obtain a result of satisfying certainty can increase rapidly and it may even be impossible to perform a meaningful measurement if the noise influence dominates the overall signal.
From a different point of view, noise sources also play a crucial role in the design of e.g. detectors, measurement devices and generally in the fabrication of electronic devices, where the demand of low power consumption is often contrary to the robustness against the influence of noise. This illustrates that sources of noise have to be characterised accurately and have to be taken into account if one has to optimize the performance or robustness of an electronic device.
In contrast to these unfavorable effects, there are also applications where noise can be used to gain information about the experimental system or even perform measurements of fundamental constants of nature. In this experiment for example, the Boltzmann constant k_B and the elementary charge e are determined on a level of accuracy of less than 1 % with respect to the current reference values. This already indicates that noise is often of very fundamental character. In case of Johnson noise, which is of thermal origin, an important application is the utilization of its temperature dependence to actually measure the temperature of a probe by monitoring the magnitude of noise it creates. This technique is often referred to as noise thermometry and is the basis of precision measurements of very large temperatures as well as very low, cryogenic temperatures [6]. A simple version of such a measurement scheme is performed as a final experiment.

3. Tasks

- Johnson noise measurements:
  - Measure the dependence of Johnson noise $\langle V_\mathrm{J}^2 \rangle$ on the source resistance R_in for a fixed ENBW Δf
  - Measure the dependence of Johnson noise $\langle V_\mathrm{J}^2 \rangle$ on the ENBW Δf for a fixed source resistance R_in

- Shot noise measurements:
  - Measure the dependence of shot noise $\langle V_{\text{shot}}^2 \rangle$ on the photocurrent I_{dc} by varying the supply voltage of the light source, keeping the ENBW Δf fixed (for bulb, LED and IR-LED)
  - Measure the dependence of shot noise $\langle V_{\text{shot}}^2 \rangle$ on the ENBW Δf, keeping the photocurrent I_{dc} fixed (for bulb, LED and IR-LED)
- Noise thermometry:
  - Match the internal probe resistance $R_{\text{in}}^{\text{int}}(T_{\text{A}})$ to the external one $R_{\text{in}}^{\text{ext}}(T_{\text{X}})$
  - Match the compensation capacity C_{comp} to the parasitic capacity of the probe cable
  - Determine the temperature of a probe immersed in liquid nitrogen $T_{\text{X}} = T_{\text{N2}}$

4. Reading material for preparation

The manufacturer (Teachspin, Inc.) provides an extensive manual (see ref. [1] or OLAT) together with their experimental apparatus. For the measurements that should be carried out here, we concentrate on some of the topics covered in this manual. The contained descriptions should give you a better understanding of the experimental setup (especially of the analysing electronics) and also contain a different approach in the introduction of different types of noise. The following list gives an overview of the topics that are (possibly) relevant for your preparation and the evaluation of the measurements (error estimates). Topics that are crucial for understanding the experiment are marked in **bold** font. These can be considered as the minimum requirements on preparation for this experiment (together with this manual).

- Noise fundamentals:
  - Techniques and quantities to characterise noise signals - **Chapter 2**
  - Johnson noise - **Chapter 1**
  - Shot noise - **Chapter 3.0 - 3.3** (p. 3-1 - p. 3-16)
  - Noise thermometry - **Chapter 6.4** (p. 6-12 - p. 6-16)
  - Gaussian noise vs. white noise - Appendix A.9 (p. A-30 - p. A-31)
  - Fluctuations in measured noise: The Dicke limit - Appendix A.12 (p. A-46 - p. A-48)
- Basic electronics:
  - Photodiodes - Chapter 3.6 & 3.7 (p. 3-26 - p. 3-31)
  - Operational amplifier (op-amp) circuits - see e.g. ref. [3]
  - Noise considerations on op-amp circuits - Appendix A.3 (p. A-6 - p. A-15)
  - The matter of a.c. or d.c. coupling - Appendix A.2 (p. A-3 - p. A-5)
- Tolerances and uncertainties:
  - Specified accuracy - Chapter 5.0 (p. 5-1 - p. 5-2)
  - Technical specifications - Appendix A.1 (p. A-1 - p. A-2)

5. Theory

5.1. Spectral noise density, voltage noise density and ENBW

Fundamental noise sources in electronic signals can in general be described by current- or voltage-signals with vanishing mean value $\langle V \rangle = 0$, but a non-vanishing fluctuation term $\langle V^2 \rangle \neq 0$. Therefore it's clear that the later mentioned expression is a measure for the magnitude of noise. However, $\langle V^2 \rangle$ only describes the overall magnitude of fluctuations, but it contains no information on spectral decomposition of the noise signal. Therefore, a more common and practical measure is the so called spectral noise density S, which is connected to $\langle V^2 \rangle$ by

$$\langle V^2 \rangle = \int_{f_1}^{f_2} S(f) \mathrm{d}f \tag{1}$$

with f_1 and f_2 the lower and upper border of the considered "brick wall" frequency window in which noise contributes to the signal (typically determined by the frequency range that the considered circuit is sensitive to). This definition is still not applicable to realistic circuits, because a "brick wall" frequency sensitivity can never be realized. A more realistic formulation is given by

$$\langle V^2 \rangle = \int_0^\infty G^2(f) S(f) \mathrm{d}f \tag{2}$$

where $G(f)$ describes the transfer function of the given circuit, defined by the ratio of the output- and input-voltage according to $G(f) = V_{\mathrm{out}}/V_{\mathrm{in}}$. This definition allows to change the limits of integration to 0 and ∞. For regions that the circuit is insensitive to, the transfer function will simply be $G = 0$.
For the special case of so called white noise, the spectral noise density is frequency independent $S(f) = S$. This allows for a reinterpretation of the definition in eq. (2). We can pull the constant factor of the spectral noise density S outside the integral and define the remaining integral as the so called equivalent noise bandwidth Δf (ENBW):

$$\Delta f = \int_0^\infty G^2(f) \mathrm{d}f. \tag{3}$$

The ENBW can be interpreted as the "brick wall" bandwidth that an ideal filter with infinitely strong damping outside its passband would need to have in order to end up with the same magnitude of time-averaged quadratic voltage fluctuations $\langle V^2 \rangle$.
Sometimes the spectral noise density is also called (spectral) noise power density. The connection to power is obtained by relating S to a resistance R (which resistance to take is typically clear from the context of the experiment). Clearly, power can be expressed as $P = V^2/R$, so the resulting quantity will have units of $\mathrm{V}^2/\Omega\mathrm{Hz} = \mathrm{W\,Hz}^{-1}$ which justifies the term noise power density.
As one is often thinking of electric signals as voltage signals, the use of the voltage noise density D is also common. This is defined via

$$D = \sqrt{S} \tag{4}$$

and leads to a somehow obscure unit for D of $\mathrm{V}/\sqrt{\mathrm{Hz}}$. However, the interpretation is straightforward if one follows the steps in the definition of S. The question of when it is useful to describe a noise signal by S and when by D may arise. The voltage noise density is especially useful for multiplications with an arbitrary transfer function as the later is defined by a relation of voltages. On the other hand, if one thinks of a superposition of noise signals, then S is the correct measure to work with. This can easily be seen by considering the mean squared voltage $\langle V^2 \rangle$. A superposition of two noise voltage signals $V_1(t)$ and $V_2(t)$ is described by

$$\langle (V_1(t) + V_2(t))^2 \rangle = \langle V_1(t)^2 \rangle + 2\langle V_1(t) V_2(t) \rangle + \langle V_2(t)^2 \rangle. \tag{5}$$

Assume that the two noise signals are not correlated, which is the case if the underlying processes that create the noise are independent. Therefore the term $\langle V_1(t)V_2(t)\rangle$ will vanish, which can be seen by considering the spectral decomposition of the two signals and assuming random phase relations between equal frequency components. Terms with different frequencies vanish for long enough averaging times and terms with equal frequencies will on average cancel each other for random phase relations. Therefore we are left with

$$\langle (V_1(t) + V_2(t))^2 \rangle = \langle V_1(t)^2 \rangle + \langle V_2(t)^2 \rangle. \tag{6}$$

For white noise sources, this implies, that also the related spectral noise densities S_1 and S_2 are additive, simply because the voltage fluctuations are confined to the same frequency range Δf.

5.2. Johnson noise

Johnson noise is named after physicist John B. Johnson, who first analyzed electrical noise in a conductor in 1926 at the Bell labs in the US [2]. In 1928, it was his colleague Harry Nyquist who put the experimental results described by Johnson on theoretical grounds [4].
In the derivation of Nyquist, the configuration is as follows: we consider a lossless line of length ℓ that is terminated on both ends I, II by resistors of resistance R, as illustrated in fig. 1.

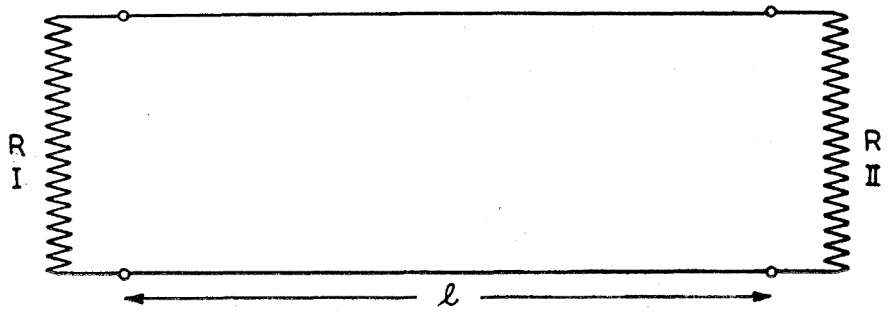

Figure 1: Experimental configuration in the Nyquist derivation of Johnson noise. Two resistors of resistance R are connected by a lossless line. *Figure adapted from ref.* [4].

From the telegrapher's equation one can find that if a line is terminated by a resistor of magnitude equal to the so called characteristic impedance of the line, waves travelling along the line are not reflected at the ends. From the perspective of the source, this is equivalent to the situation that an infinitely long line has been connected, where the outgoing travelling wave is never reflected.

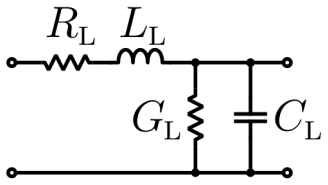

Figure 2: Transmission line element. *Figure adapted from ref.* [7].

For the characteristic impedance Z_0 of a two-wire line segment of the form in fig. 2 one finds

$$Z_0 = \sqrt{\frac{R_\mathrm{L} + i\omega L_\mathrm{L}}{G_\mathrm{L} + i\omega C_\mathrm{L}}}. \tag{7}$$

All the variables in this relation carry an index L to illustrate that they are defined as quantities per unit length L. Here, R_L is the resistance of the wires, G_L the conductance of the dielectric separating the wires, L_L the inductance and C_L the capacity of the line segment. The line can therefore be seen as a series of infinitesimal segments. This implies, that in order to get e.g. the resistance of the whole line the value R_L has to be multiplied by the length of the line ℓ. However, for a homogeneous medium with constant factors R_L, G_L, L_L and C_L, the characteristic impedance is the same for any length ℓ of the line.
In our model, we consider a lossless line ($R_\mathrm{L} = 0$, $G_\mathrm{L} = 0$) with a characteristic impedance of $Z_0 = R$, equal to the resistance of the terminating resistors at each end of the line,

$$Z_0 = \sqrt{\frac{L_\mathrm{L}}{C_\mathrm{L}}} = \sqrt{\frac{L}{C}} \stackrel{!}{=} R. \tag{8}$$

The reflection coefficient is described by

$$r = \frac{Z - Z_0}{Z + Z_0}, \tag{9}$$

with Z being the terminating impedance connected to the considered end of the line and Z_0 the characteristic impedance. In our configuration with $Z = R = Z_0$, a wave entering on one side travels across the line and is terminated by the resistor on the other end. Therefore the wave doesn't cause any reflection in the opposite direction and deposits its whole energy in the terminating resistor.
The thermal agitation of charge carriers in a conductor creates current fluctuations. On average, these fluctuations are zero ($\langle I \rangle = 0$), however the squared current has an average value $\langle I^2 \rangle \neq 0$. According to this, also the transferred power $\langle P \rangle = \langle I^2 \rangle \cdot R \neq 0$. However, because the two resistors are connected by a lossless line, the resistors establish a thermal equilibrium. The second law of thermodynamics therefore states, that in thermal equilibrium the power flowing from the first resistor to the second is equal to the power flowing from the second to the first. This statement can be made even more rigorous by ignoring the lossless line for a moment and instead adding a non-dissipative LC resonator section between the two directly connected resistors, as shown in fig. 3.

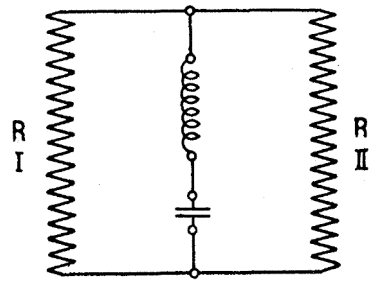

Figure 3: LC resonator as frequency selective element. *Figure adapted from ref.* [4].

The resonator effectively restricts the power transport to a certain frequency window. Still the circuit is in thermal equilibrium, so also the power transport in the restricted frequency band has to be equal in both directions in order to fulfil the second law of thermodynamics. This consideration leads to the result that the power exchange has to follow a detailed balance situation for any infinitesimal frequency range from ν to $\nu + \mathrm{d}\nu$. This can also be formulated in the following way

$$\langle \Pi_{\mathrm{I}\to\mathrm{II}}(\nu) \rangle \mathrm{d}\nu = \langle \Pi_{\mathrm{II}\to\mathrm{I}}(\nu) \rangle \mathrm{d}\nu \tag{10}$$

with $\Pi(\nu)$ being the power spectral density and the indices representing the direction of power transport.
With this result in mind, we return to the situation with the lossless line as connection of the two

resistors. Let the temperature of the system be T, the length of the line be ℓ and the velocity of wave propagation across the line be v. Imagine the following situation: the system of line and resistors is in thermal equilibrium. Now we instantaneously disconnect the resistors and simultaneously short the ends of the line, such that $Z = 0$ and according to eq. (9) the waves undergo a total reflection at the ends of the line. The energy that the travelling waves transported is now trapped. Instead of describing the voltage waves across the line as travelling waves, we can now look at the superposition of the travelling waves in opposite propagation directions and find that a standing wave with nodes at both ends of the line is created. The possible wavelengths λ_n of the standing wave for these boundary conditions are

$$\lambda_\mathrm{n} = \frac{2\ell}{n} \tag{11}$$

with $n \in \mathbb{N}$ an arbitrary integer number. Via the propagation velocity c_v, these wavelengths can be translated into frequencies, using the relation $c_\mathrm{v} = \lambda \cdot \nu$. The mode frequency of the n-th mode therefore is

$$\nu_\mathrm{n} = n\frac{c_\mathrm{v}}{2\ell}. \tag{12}$$

If we now consider a frequency range from ν to $\nu + \mathrm{d}\nu$, the number of modes in this range can be obtained by calculating the corresponding density of mode frequencies

$$D(\nu) = \frac{1}{c_\mathrm{v}/2\ell} = \frac{2\ell}{c_\mathrm{v}} \tag{13}$$

which in this case is simply given by the inverse of the spacing between two neighbouring modes in this 1D problem. The energy per mode is described by the Planck formula in the present case, given by

$$\langle E_\nu\rangle \mathrm{d}\nu = \frac{h\nu}{\exp\left(\frac{h\nu}{k_\mathrm{B}T}\right) - 1}\mathrm{d}\nu \approx k_\mathrm{B}T\mathrm{d}\nu, \tag{14}$$

where in the approximate result we developed the exponential for small arguments $h\nu/k_\mathrm{B}T$, which is fulfilled in most relevant cases for electronic circuits.
The energy density is obtained accordingly

$$D(\nu)\langle E_\nu\rangle \mathrm{d}\nu = \frac{2\ell}{c_\mathrm{v}}k_\mathrm{B}T\mathrm{d}\nu. \tag{15}$$

This energy is equivalent to the power emitted to the line by the two resistors during the passage time across the line of ℓ/c_v. Therefore the power spectral density of a single resistor is given by

$$\langle P(\nu)\rangle \mathrm{d}\nu = k_\mathrm{B}T\mathrm{d}\nu. \tag{16}$$

If we now connect this result to the relation $\langle P\rangle = \langle I^2\rangle R$ and consider that the current I in the circuit is connected to the voltage V by $I = V/2R$, we find:

$$\langle P\rangle \mathrm{d}\nu = k_\mathrm{B}T\mathrm{d}\nu = \langle I^2(\nu)\rangle R\mathrm{d}\nu = \frac{\langle V^2(\nu)\rangle}{4R^2}R\mathrm{d}\nu, \tag{17}$$

$$\tag{18}$$

$$\langle V^2(\nu)\rangle \mathrm{d}\nu = 4k_\mathrm{B}TR\mathrm{d}\nu \qquad \longrightarrow \qquad \langle V_\mathrm{J}^2\rangle = 4k_\mathrm{B}TR\Delta\nu. \tag{19}$$

Here eq. (19) describes the Johnson noise voltage fluctuations caused by a resistance R. Furthermore, if we want to express the Johnson noise from <u>one</u> resistor in form of current fluctuations, we find:

$$\langle I^2(\nu)\rangle \mathrm{d}\nu = \frac{\langle V^2(\nu)\rangle}{R^2}\mathrm{d}\nu = \frac{4k_\mathrm{B}T}{R}\mathrm{d}\nu \qquad \longrightarrow \qquad \langle I_\mathrm{J}^2\rangle = \frac{\langle V_\mathrm{J}^2\rangle}{R^2} = \frac{4k_\mathrm{B}T}{R}\Delta\nu. \tag{20}$$

In an equivalent circuit, these noise measures can be modelled with a voltage- or current-source in combination with a noiseless resistor, which is illustrated in fig. 4.

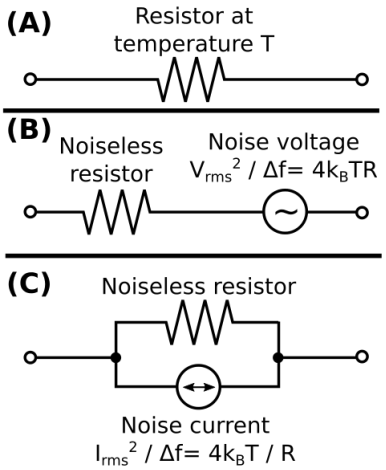

Figure 4: Equivalent circuits for a Johnson noise source. The quantities V_{rms}^2 and I_{rms}^2 correspond to $\langle V_{\mathrm{J}}^2 \rangle$ in eq. (19) and $\langle I_{\mathrm{J}}^2 \rangle$ in eq. (20) respectively. *Figure adapted from ref.* [8].

Finally, the resulting spectral noise density defined in section 5.1 for Johnson noise is equal to

$$S_{\mathrm{J}} = 4k_{\mathrm{B}}TR. \tag{21}$$

5.3. Shot noise

Shot noise is a direct consequence of charge quantization. Since the charge can only be transferred in units of the elementary charge e and the instantaneous current can be written as

$$i = \frac{\mathrm{d}Q(t)}{\mathrm{d}t} = e\frac{\mathrm{d}N(t)}{\mathrm{d}t}, \tag{22}$$

with $N(t)$ being the total number of transferred electrons, we find for the average current I in a time of Δt, that it is equivalent to

$$I(\Delta t) = \frac{e}{\Delta t}\int_0^{\Delta t}\frac{\mathrm{d}N}{\mathrm{d}t}\mathrm{d}t = \frac{e}{\Delta t}n(\Delta t), \tag{23}$$

with $n(\Delta t)$ the number of transferred electrons in a time Δt. This number $n(\Delta t)$ is subject to fluctuations, that are determined by the fundamental nature of the current.
To consider the fluctuations in the average current I, we have to look at the variance σ_{I}^2 of the average current value

$$\sigma_{\mathrm{I}}^2 = \langle (I - \langle I \rangle)^2 \rangle = \langle I^2 \rangle - \langle I \rangle^2, \tag{24}$$

where the symbol $\langle ... \rangle$ should be understood as taking the average over a sample of point measurements of the average current. In an actual experiment we would acquire these point measurements of the average current I_i by taking the time-average of the momentary current over a time span of Δt. The values of the point measurements I_i can now be treated as random samples of an underlying distribution, ignoring the fact that they are related to a certain averaging-time for a moment. We rewrite the variance in the form

$$\sigma_{\mathrm{I}}^2 = \frac{1}{N}\sum_{i=1}^{N}\left(I_i - \bar{I}\right)^2, \tag{25}$$

with $\bar{I} = \langle I \rangle$ being the expectation value of the underlying distribution of the current point measurements. The two quantities for the average current in the above relation can also be written in terms of the number of transferred electrons according to

$$I_i(\Delta t) = n_i(\Delta t)\frac{e}{\Delta t}, \tag{26}$$

$$\bar{I}(\Delta t) = \bar{n}\frac{e}{\Delta t}, \tag{27}$$

with $n_i(\Delta t)$ the number of electrons for the particular point measurement and $\bar{n}$ the average number of electrons. If the arrival of any two electrons is statistically independent and therefore completely uncorrelated, this number $n(\Delta t)$ is subject to fluctuations according to Poisson statistics, which predicts that $\sigma_\mathrm{n} = \sqrt{\bar{n}}$. Assuming this, we can rewrite eq. (25) in terms of fluctuations in the number of electrons:

$$\sigma_\mathrm{I}^2 = \frac{1}{N}\sum_{i=1}^{N}\left(I_i - \bar{I}\right)^2 = \frac{e^2}{N\Delta t^2}\sum_{i=1}^{N}\left(n_i - \bar{n}\right)^2 = \tag{28}$$

$$= \frac{e^2}{\Delta t^2}\sigma_\mathrm{n}^2 = \frac{e^2}{\Delta t^2}\bar{n} = \frac{e}{\Delta t}\bar{I}. \tag{29}$$

From this result, we can calculate the expectation value for the quadratic current fluctuation term, which we define as

$$\langle \delta I^2 \rangle := \langle \left(I - \bar{I}\right)^2 \rangle = \sigma_\mathrm{I}^2 = \frac{e}{\Delta t}\bar{I}. \tag{30}$$

The averaging time can further be expressed by the bandwidth Δf that the experimental setup is sensitive to, via the Shannon-Nyquist theorem $\Delta t = (2\Delta f)^{-1}$ (with Δf equivalent to the ENBW defined in eq. (3)). This results in the well known Schottky formula [5] for shot noise in electrical currents, described by

$$\langle \delta I^2 \rangle = 2e\Delta f\bar{I}. \tag{31}$$

Because the term $\langle \delta I^2 \rangle / \Delta f$ only has to be related to a resistance R (resulting from the specific circuit) to receive a quantity with units of the ones of a spectral noise density, the definition

$$S_\mathrm{shot} = \frac{\langle \delta I^2 \rangle}{R^2 \Delta f} = 2e\frac{\bar{I}}{R^2} \tag{32}$$

can be made, with S_shot the spectral noise density of shot noise. From this result it can directly be seen that shot noise describes a white noise source, because $\bar{I}$ and R are frequency independent quantities.

6. Measurement protocol

6.1. Johnson noise measurements

Dependence on resistance R_{in}:
Configure the LLE unit as depicted in fig. 5 and fig. 6. Measure the resulting output voltages V_{out} of the time-averaging section of the HLE unit for the available resistance values of R_{in}. As a setting of the filter stages you can e.g. choose $f_{\mathrm{c,HP}} = 0.1\,\mathrm{kHz}$ and $f_{\mathrm{c,LP}} = 10\,\mathrm{kHz}$. Optimize the HLE gain G_{HLE} for every measurement point to receive an output voltage in the range of $V_{\mathrm{out}} = 0.2 - 0.5\,\mathrm{V}$. Extrapolate the lower end of the $\langle V^2 \rangle$ data series to a resistance $R_{\mathrm{in}} = 0$ to determine $\langle V_{\mathrm{amp}}^2 \rangle$ and correct the measurements. Check if the obtained $\langle V_{\mathrm{J}}^2 \rangle$ values can be described by the presented theory, according to eq. (19). Give an estimate for the Boltzmann constant k_{B} from a fit to your data points.

Dependence on ENBW Δf:
The LLE unit remains in the same configuration of the earlier measurements on resistance dependence. For a fixed value of R_{in} of your choice (consider the effect of parasitic capacitances of $\approx 10\,\mathrm{pF}$ that are present in every real resistor) measure the HLE output voltage V_{out} for different values of the ENBW Δf, i.e. for different combinations of filter corner frequencies $f_{\mathrm{c,HP}}$ and $f_{\mathrm{c,LP}}$. Keep in mind that every measurement has to be corrected for amplifier noise by a dark measurement. Therefore, try not to measure too many filter combinations but rather concentrate on a selection that covers a large range of ENBW values Δf. To speed up the measurement procedure, the dark measurements are performed by simply using the obtained value for $R_{\mathrm{in}} = 10\,\Omega$ as an approximation for $R_{\mathrm{in}} \to 0$. Check if the results for $\langle V_{\mathrm{J}}^2 \rangle$ are in agreement with theory and repeat the calculation of the Boltzmann constant k_{B}.

6.2. Shot noise measurements

Dependence on photocurrent I_{dc}:
For the measurements on the light bulb, the LLE unit has to be changed to the configuration in fig. 8, whereas for the case of the LED and IR-LED fig. 10 illustrates the suitable configuration. Set the feedback resistor to $R_{\mathrm{f}} = 10\,\mathrm{k}\Omega$ and use a series resistor of $R_{\mathrm{s}} = 1\,\mathrm{k}\Omega$ for the LED and IR-LED. Record the voltage levels of the HLE output V_{out} and the monitor output V_{mon} of the I-to-V-converter for different values of the supply voltage of the light source, always adjusting the HLE gain G_{HLE} in the way described above for the Johnson noise measurements. V_{mon} should not considerably exceed a level of 1 V. Place the LLE unit on a foam mat throughout the experiment to reduce the influence of mechanical vibrations. For the LED and IR-LED you should ensure that the maximum current is not exceeded by monitoring the voltage drop across the series resistor via the provided monitor port. However, disconnect the digital multimeter (DMM) from this monitor port for every measurement point you take to avoid environmental noise to couple to your light supply circuit. Subtract the $\langle V^2 \rangle$ value obtained from a dark measurement from the other measurement points. Also the values of V_{mon} have to be corrected by the value obtained in the dark measurement, which is typically small but non-zero. Test the predictions of eq. (31) with your acquired data and calculate an estimate for the elementary charge e.
Additionally, you should acquire Fourier spectra (FFT measurement) of the output voltage of the LLE unit for a few interesting settings and compare the different light sources. This is achieved by directly measuring the V_{mon} signal with a spectrum analyser, which allows you to directly measure the spectral noise density (how?) and possibly identify deviations from the theoretical white noise behaviour in form of detrimental additional noise sources.

Dependence on ENBW Δf:
We keep the same configuration of the LLE setup as in the earlier shot noise measurements on photocurrent dependence. Set the supply voltage of the light source to a level that produces a moderate monitor voltage V_{mon} at the output of the I-to-V-converter in a range of $\approx 300 - 600\,\mathrm{mV}$. Take measurements of the output voltage level V_{out} of the HLE section for different choices of the filter corner frequencies for all three different light sources. You will observe deviations from the expected white noise behaviour if you choose a pass-band of the filter combination in the low frequency range, especially if the LED or IR-LED is used as light source. This behaviour should also be visible in the Fourier spectra that were acquired in the first shot noise measurement. For a further estimate of the elementary charge e, it is advantageous to exclude this low frequency range from the measurements by setting the high-pass filter corner frequency to $f_{\mathrm{c,HP}} = 1\,\mathrm{kHz}$ or $f_{\mathrm{c,HP}} = 3\,\mathrm{kHz}$ and only vary the low-pass corner frequency $f_{\mathrm{c,LP}}$.

6.3. Noise thermometry

Matching the probe resistances $R_{\mathrm{in}}^{\mathrm{int}}(T_{\mathrm{A}}) \longleftrightarrow R_{\mathrm{in}}^{\mathrm{ext}}(T_{\mathrm{X}})$:
Prepare the LLE unit in the configuration illustrated in fig. 12 ($R_{\mathrm{in}}^{\mathrm{int}}$ and C_{comp} will be added later). Measure the resistance between the GND port and the A_{ext}, B_{ext} and C_{ext} port with a DMM and the break-out-box and determine which of the ports of the probe cable is connected to the probe resistor with a nominal resistance of $10\,\mathrm{k\Omega}$. If the probe cable is connected to the LLE unit, the external resistor probe is selected via the corresponding setting of the R_{in} selector switch. Place the glass dewar in the designated holder and fill it with liquid nitrogen. Now lower the probe until the cold finger (made out of brass) is completely immersed. Wait until the probe has thermalized with the liquid nitrogen bath, which is the case when the boiling ceases. If one wants to be sure that the probe has thermalized, one can also monitor the output voltage V_{out} of the HLE section during the cool down process. You will be able to see the output voltage drop continuously until it settles at a certain value, which is the indication that the probe has reached the liquid nitrogen temperature. Finally, measure the resistance between the relevant pins of the R_{in} selector switch at the back of the LLE circuit board to determine $R_{\mathrm{in}}^{\mathrm{ext}}(T_{\mathrm{X}})$. This is the value that the resistance of the internal reference resistor $R_{\mathrm{in}}^{\mathrm{int}}(T_{\mathrm{A}})$ should have at ambient temperature. Insert the reference resistor $R_{\mathrm{in}}^{\mathrm{int}}$ in the screw terminal of the C_{ext} port of the R_{in} selector switch.

Matching the compensating capacitance C_{comp} to the parasitic probe cable capacitance:
The probe cable effectively adds a parasitic capacitance in parallel to the external probe resistor $R_{\mathrm{in}}^{\mathrm{ext}}$. To assimilate the way that the two probe resistors act in the I-to-V-converter circuit, we also have to add a compensation capacitor C_{comp} in parallel to the internal reference resistor to mimic the behaviour of the external probe resistor $R_{\mathrm{in}}^{\mathrm{ext}}$. This R-C-combination describes a low-pass filter in principle. Hence, we simply have to compare the resulting output voltages V_{out} for both probe resistors in different frequency regions by choosing different corner frequencies for the filters. Repeat this measurement for several choices of the compensation capacity C_{comp} until no difference in the resulting output voltages for the two probe resistors can be observed. A good starting point for C_{comp} is typically $C_{\mathrm{comp}} \approx 100\,\mathrm{pF}$. You can also check if the matching procedure was successful by acquiring FFT measurements for the I-to-V-converter output V_{mon} for both probe resistors. Ideally, also perform a FFT measurement without the compensation capacitor for comparison.
In order to save some liquid nitrogen, the measurements can be carried out with a different internal reference resistor $R_{\mathrm{in}}^{\mathrm{int}}(T_{\mathrm{A}})$ that is matched to the resistance of the external one $R_{\mathrm{in}}^{\mathrm{ext}}(T_{\mathrm{A}})$ at ambient temperature.

Determination of the boiling temperature of liquid nitrogen $T_X = T_{N2}$:
Connect the internal reference resistor R_{in}^{int} and the compensation capacitor C_{comp} dimensioned in the former measurements to the C_{ext} screw terminal according to fig. 12. Again immerse the external probe resistor R_{in}^{ext} in liquid nitrogen and wait until it has thermalized. Now raise the level of shot noise contribution to the signal of the external probe until it reaches the signal level of the internal probe resistor without added shot noise. You can compute the temperature difference of the two resistor probes from the voltage output of the I-to-V-converter V_{mon}, according to

$$\frac{k_B}{e} \cdot (T_A - T_X) = \frac{1}{2} R_{in} \cdot I_{shot} = \frac{1}{2} R_{in} \cdot \left(\frac{-V_{mon}}{R_f} \right), \tag{33}$$

Is the calculated temperature in agreement with reference values in the literature? If not, can you think of imperfections in the experimental setup or detrimental influences that can account for the deviation?

7. Error analysis

The following section presents estimated uncertainties for the specific apparatus that you will be working on. The uncertainties that are not covered here can be found in the chapters on tolerances and uncertainties in the manual [1] (see section 4).
Uncertainties in the function of the squarer and time-averaging section were checked via calibration measurements and can be neglected in comparison to the dominant uncertainties of gain factors and ENBW values.

7.1. Uncertainties in gain factors

The manual of the commercially sold experiment states an uncertainty for the amplification factor G_J of the non-inverting amplifier of 0.2 %, which takes into account the uncertainties in resistor values that set the gain factor and the frequency dependence of the gain response of the OPA-134 operational amplifier.
The amplification factor of the HLE gain section is controlled via the setting of two multiplicator switches with a choice of a x1 or x10 magnification and a rotary switch that selects the fine gain value in a range of $10 - 100$, resulting in a accessible range for the HLE gain of $10 - 10\,000$. The two multiplicators as well as the fine gain selection are subject to an uncertainty of $G_{mult} = G_{fine} = 0.2\,\%$ respectively. An overview on uncertainties in amplification factors is presented in table 1.

Amp. section	Uncertainty
$G_J = 6$	$\Delta G_J / G_J = 0.2\,\%$
$G_{pre-amp} = 100$	$\Delta G_{pre-amp} / G_{pre-amp} = 0.4\,\%$
$G_{mult} = 1$ or 10	$\Delta G_{mult} / G_{mult} = 0.2\,\%$
$G_{fine} = 1 - 100$	$\Delta G_{fine} / G_{fine} = 0.2\,\%$
LLE section	HLE section
$G_{LLE} = \begin{cases} G_J \cdot G_{pre-amp} & \text{Johnson n.} \\ G_{pre-amp} & \text{Shot n.} \end{cases}$	$G_{HLE} = G_{mult,1} \cdot G_{mult,2} \cdot G_{fine}$

Table 1: Gain factors and connected uncertainties specified by the manufacturer TeachSpin, Inc. [1].

7.2. Filter ENBW uncertainty

As described in section 5.1, the quantity of the ENBW Δf plays a crucial role in noise measurements. In the present setup, the transfer function is determined by the selected filter configuration, which in our case is a combination of a high-pass filter with a small corner frequency $f_{\mathrm{c,HP}}$ and a low-pass filter with a larger corner frequency $f_{\mathrm{c,LP}}$. The filters are implemented by active second order Butterworth-type filters, which can be modelled by three parameter transfer functions of the form

$$G_{\mathrm{LP}}(f) = \frac{g}{\sqrt{\left(1-(f/f_{\mathrm{c,LP}})^2\right)^2 + (2\gamma f/f_{\mathrm{c,LP}})^2}}, \tag{34}$$

$$G_{\mathrm{HP}}(f) = \frac{g\,(f/f_{\mathrm{c,HP}})^2}{\sqrt{\left(1-(f/f_{\mathrm{c,HP}})^2\right)^2 + (2\gamma f/f_{\mathrm{c,HP}})^2}}. \tag{35}$$

Here g is the pass-band amplification of the active filter and γ is the damping parameter of the filter. For the ideal case of a Butterworth-characteristic of the filter, $g = 1$ and $\gamma = 1/\sqrt{2}$. In our case the pass-band gain is subject to an uncertainty of $g = 1.000(3)$. The value of the damping parameter depends on the chosen corner frequency and underlies a relative uncertainty of 0.2 %. The corner frequency itself is determined by resistor values R_1, R_2 and capacitor values C_1, C_2 in the circuit of the second order active filters and results in

$$f_{\mathrm{c}} = \frac{1}{2\pi\sqrt{R_1 R_2 C_1 C_2}}. \tag{36}$$

The precision resistors used in these circuits have a tolerance of $\Delta R/R = 0.1\,\%$, whereas the capacitor values underlie an uncertainty of $\Delta C/C = 1\,\%$. From this you can then calculate the relative uncertainties $\Delta f_{\mathrm{c}}/f_{\mathrm{c}}$ for the corner frequencies of the filters.
The provided measured values from a calibration of the corner frequencies carried out by the manufacturing company are presented in table 2 as well as the determined damping parameters γ.

nominal corner frequency	meas. corner freq. $f_{\mathrm{c,HP}}$/[kHz]	damping param. γ	Nominal corner frequency	meas. corner freq. $f_{\mathrm{c,LP}}$/[kHz]	damping param. γ
0.01	0.00998	0.707	0.33	0.3338	0.708
0.03	0.02993	0.707	1	1.001	0.708
0.1	0.0998	0.707	3.3	3.336	0.707
0.3	0.2993	0.707	10	10.003	0.7055
1	0.998	0.707	33	33.27	0.6988
3	2.993	0.706	100	99.15	0.6777

Table 2: Measured values for the corner frequencies f_{c} and damping parameters γ of the filter sections of the HLE unit. The calibration measurements have been carried out by the manufacturer TeachSpin, Inc. [1].

From these measured values and estimated uncertainties, one can now determine the ENBW Δf according to eq. (3) by a numerical integration. Think of a technique to estimate the uncertainties connected to the numerically calculated ENBW values, based on the known uncertainties for the two times three free parameters $g_{\mathrm{HP/LP}}$, $f_{\mathrm{c,HP/LP}}$ and $\gamma_{\mathrm{HP/LP}}$.

Hint: One very simple but also imprecise approach to estimate the connected uncertainties is to choose the input parameters y_i from the range of $x_i \pm \sigma_i$ (with x_i labelling a free parameter and

σ_i the connected uncertainty) such that you find combinations that result in a maximum ENBW $\Delta f_{\max}$ and minimum ENBW $\Delta f_{\min}$. You can then estimate the uncertainty by simply assigning

$$\sigma_{\Delta \mathrm{f}} = \frac{\Delta f_{\max} - \Delta f_{\min}}{2} \tag{37}$$

to the standard deviation of the ENBW $\sigma_{\Delta \mathrm{f}}$. For the purpose of the measurements that are carried out in this experiment, the accuracy obtained from this method is sufficient.
If one needs a better estimate for the real uncertainty, one would have to perform a Monte Carlo simulation with the free parameters chosen randomly from the particular underlying Gaussian uncertainty distribution, iterate this process and make a histogram of the resulting ENBW values.

A. Circuits and wiring diagrams

This section presents the relevant circuit and wiring diagrams for the measurements that should be carried out, adapted from the TeachSpin manual [1]. The circuit diagrams are listed without any further description and should be useful as guidance for changes in the configuration between different measurements.

A.1. Johnson noise measurements

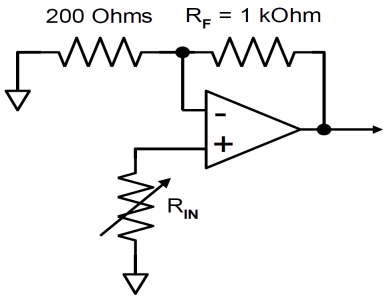

Figure 5: Circuit of a non-inverting amplifier for Johnson noise measurements. The ratio of the feedback resistor R_f and the 200 Ω resistor determines the gain for the noise signal caused by R_in. *Figure adapted from ref.* [1].

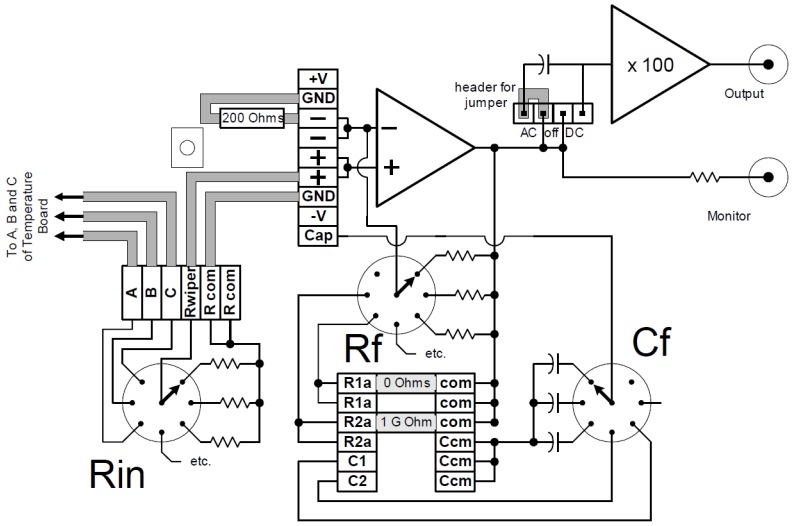

Figure 6: Wiring diagram for Johnson noise measurements. The selection switches for the setting of R_in and R_f are shown, as well as the screw terminals in which the 200 Ω precision resistor should be wired. The selection switch for C_f is irrelevant for the measurements that are described in this report. Furthermore, the jumper in front of the pre-amplifier should always be put to AC coupling. *Figure adapted from ref.* [1].

A.2. Shot noise measurements

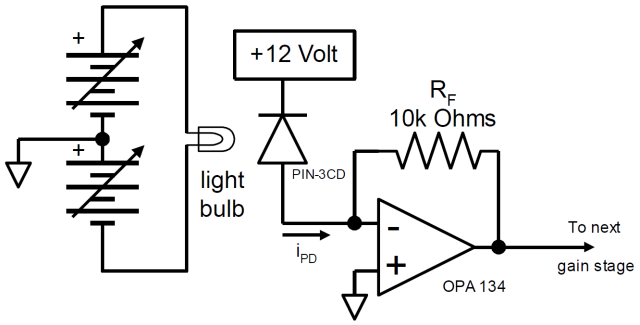

Figure 7: Circuit of a transimpedance amplifier (TIA) configuration of an OP-AMP. The photodiode is operated in reverse-bias configuration with a constant bias voltage of $-12\,\mathrm{V}$ (viewed from the perspective of the diode) and is illuminated by a bulb as light source whose light intensity can be tuned by varying its supply voltage. The photodiode current I_{PD} depends on the light intensity and therefore the fluctuations in the light intensity are translated into fluctuations of the output voltage of the TIA. *Figure adapted from ref.* [1].

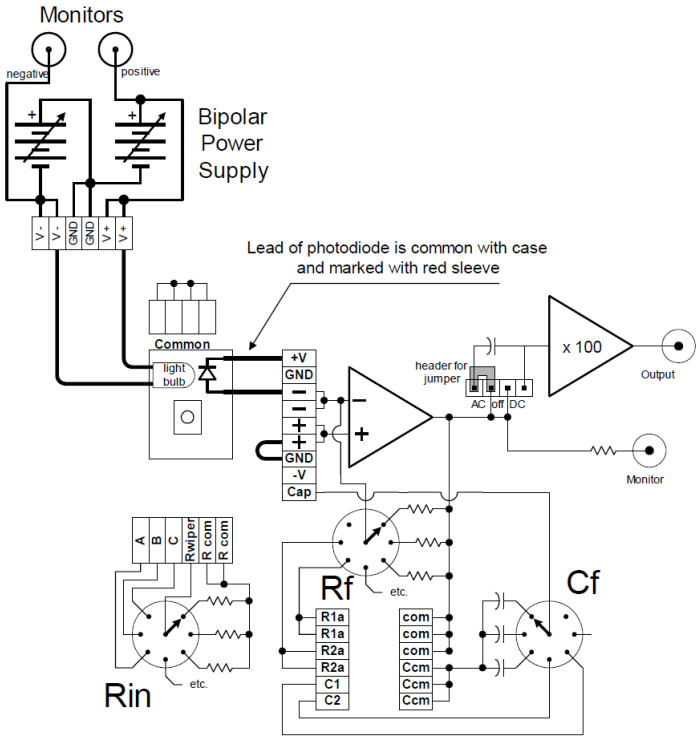

Figure 8: Wiring diagram for shot noise measurements with the bulb as light source. *Figure adapted from ref.* [1].

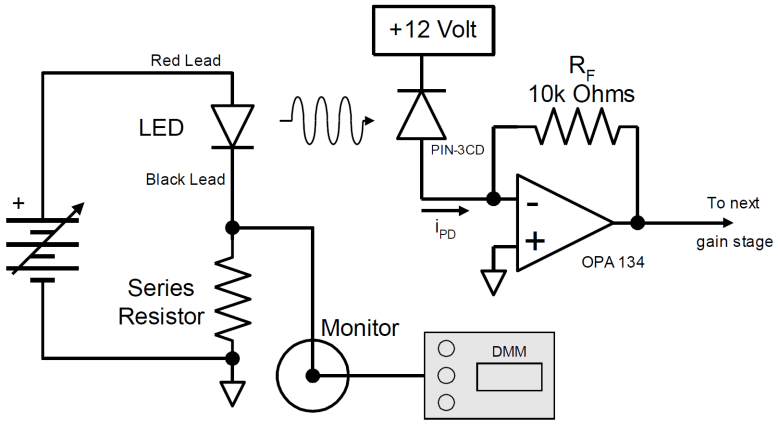

Figure 9: Modified circuit of a TIA for an LED or IR-LED as light source. The voltage drop across the series resistor R_s in the supply circuit can be measured by a digital multimeter (DMM) to monitor the LED current. *Figure adapted from ref.* [1].

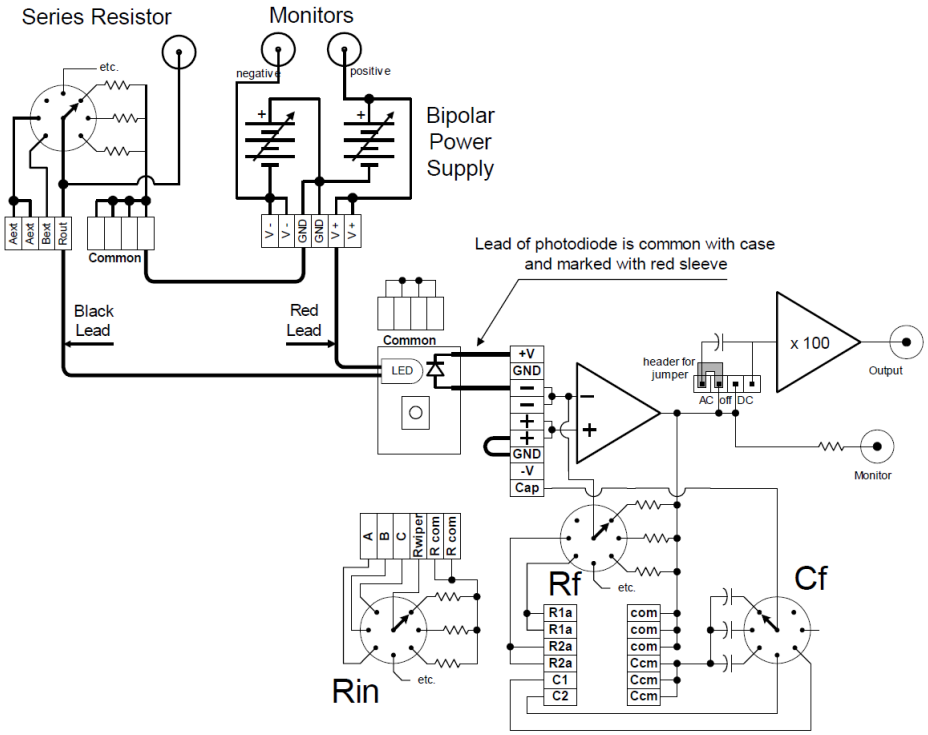

Figure 10: Wiring diagram for shot noise measurements with the LED or the IR-LED as light source. *Figure adapted from ref.* [1].

Remark: It is important that the monitoring DMM in the LED and IR-LED configuration of the shot noise setup (fig. 9) is disconnected for actual measurements. Otherwise additional noise is introduced to the system and the measurement results are distorted.

A.3. Noise thermometry

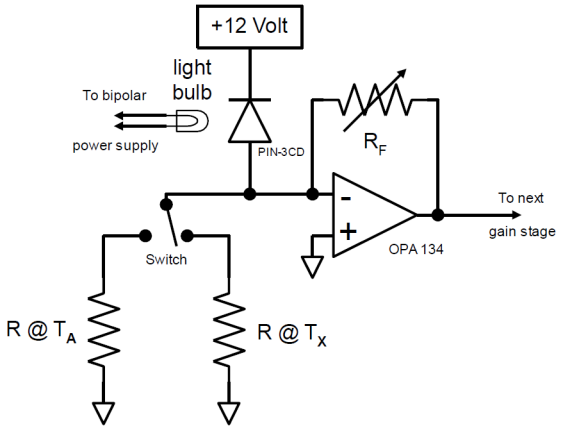

Figure 11: Circuit for noise thermometry measurements. *Figure adapted from ref.* [1].

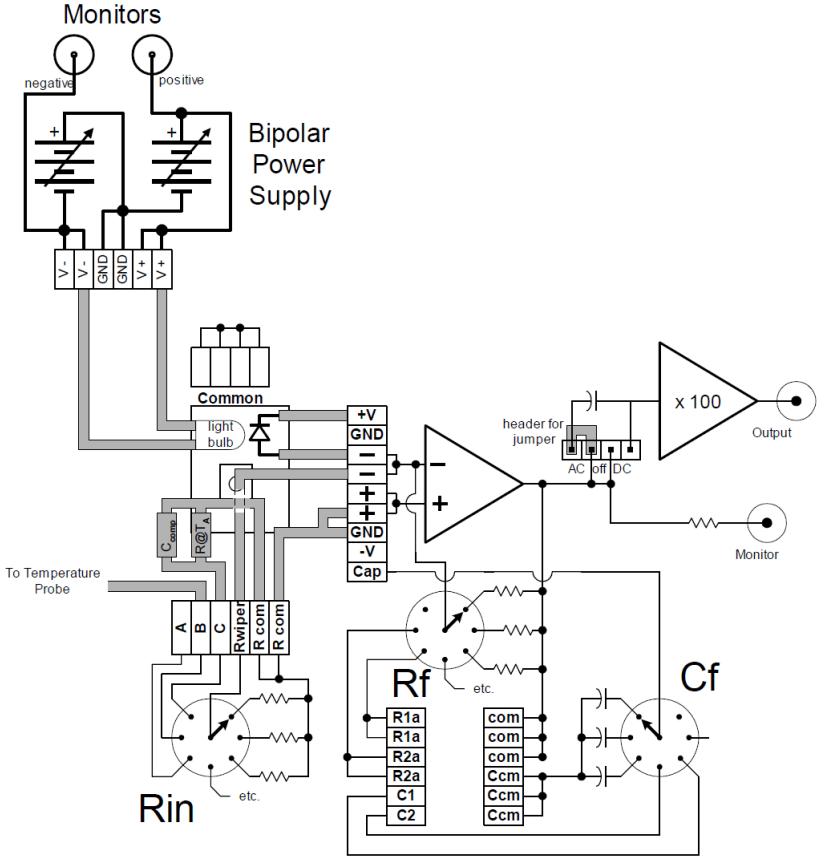

Figure 12: Wiring diagram for noise thermometry measurements. The internal probe resistor $R_{\mathrm{in}}^{\mathrm{int}}$ corresponds to $R@T_{\mathrm{A}}$ in the wiring diagram. The connection to the external probe resistor $R_{\mathrm{in}}^{\mathrm{ext}}$ is only indicated by a broken line. *Figure adapted from ref.* [1].

References

[1] Baak, David V.: *Noise Fundamentals NF1-A INSTRUCTORS MANUAL*. 1. 2495 Main Street, Suite 409, Buffalo, NY 14214-2153: TeachSpin, Inc. (Veranst.), 9 2010. – URL http://balin.cwru.edu/InstructorInformation/ExperimentNotes/NoiseFundamentals?action=AttachFile&do=view&target=TeachSpin_Noise_Fundamentals_Manual.pdf

[2] Johnson, J. B.: Thermal Agitation of Electricity in Conductors. In: *Phys. Rev.* 32 (1928), Jul, S. 97–109. – URL http://link.aps.org/doi/10.1103/PhysRev.32.97

[3] Nave, C.R.: *HyperPhysics - Op-amp Varieties*. – URL http://hyperphysics.phy-astr.gsu.edu/hbase/electronic/opampvar.html. – Georgia State University - Department of Physics and Astronomy

[4] Nyquist, H.: Thermal Agitation of Electric Charge in Conductors. In: *Phys. Rev.* 32 (1928), Jul, S. 110–113. – URL http://link.aps.org/doi/10.1103/PhysRev.32.110

[5] Schottky, W.: Über spontane Stromschwankungen in verschiedenen Elektrizitätsleitern. In: *Annalen der Physik* 362 (1918), Nr. 23, S. 541–567. – URL http://dx.doi.org/10.1002/andp.19183622304. – ISSN 1521-3889

[6] White, D R. ; Galleano, R ; Actis, A ; Brixy, H ; Groot, M D. ; Dubbeldam, J ; Reesink, A L. ; Edler, F ; Sakurai, H ; Shepard, R L. ; Gallop, J C.: The status of Johnson noise thermometry. In: *Metrologia* 33 (1996), Nr. 4, S. 325. – URL http://stacks.iop.org/0026-1394/33/i=4/a=6

[7] Wikipedia: *Transmission line element*. 04 2007. – URL https://en.wikipedia.org/wiki/Characteristic_impedance. – in article Characteristic impedance (modified)

[8] Wikipedia: *Johnson Nyquist equivalent circuits*. 09 2013. – URL https://en.wikipedia.org/wiki/Johnson%E2%80%93Nyquist_noise. – in article Johnson-Nyquist noise